This is a repository copy of *Seismic rehabilitation of substandard R.C. buildings with masonry infills*.

White Rose Research Online URL for this paper:
https://eprints.whiterose.ac.uk/125434/

Version: Accepted Version

Article:

Seismic rehabilitation of substandard R.C. buildings with masonry infills

Stylianos I. Pardalopoulos

Institute of Engineering Seismology and Earthquake Engineering, Thessaloniki, Greece

Corresponding author - e-mail: stylpard@gmail.com

Stavroula J. Pantazopoulou

Department of Civil Engineering, Lassonde Faculty of Engineering, York University, Toronto, Canada

Georgia E. Thermou

Department of Civil Engineering, Aristotle University of Thessaloniki, Thessaloniki, Greece (on leave)
Civil and Structural Engineering Department, The University of Sheffield, Sheffield, UK

Seismic rehabilitation of substandard R.C. buildings with masonry infills

Seismic deformation demands are localized in areas of stiffness discontinuity, such as in soft-storeys of frame structures, where disproportionate damage is often reported in post-earthquake reconnaissance. In many parts of the world this damage pattern is mitigated using strengthening schemes that include addition of stiffness in the structure so as to limit the magnitude of drift demands. A low-cost retrofitting method is the addition of masonry infills to increase the stiffness of soft storeys in low- to mid-rise reinforced concrete (R.C.) structures. This is an easily replaceable remedy in the event of damage that may prove advantageous over R.C. structural systems, owing to the lower forces imparted to the foundation in this retrofit option as compared to more thorough interventions, thereby avoiding extensively invasive retrofit operations in the foundation. Behavioural mechanisms mobilized by masonry infills in successful retrofits are shown to emulate confined masonry behaviour. It is also shown that despite their brittleness, well connected infills can successfully mitigate the occurrence of catastrophic damage by diverting damage localization from the vulnerable regions of the building. The main objective of the current paper is to present a rapid retrofit design methodology, where masonry infills are utilized for strengthening existing substandard constructions in order for their R.C. load bearing elements to behave elastically in the event of the design earthquake. To facilitate the retrofit design, practical design charts have been derived, to link drift demand to the ratios of infills' area in plan to the total plan area in the critical floor of the structure. Performance criteria, such as target distributions of interstorey drift demand, a target estimate of the fundamental period, as required by the designer, and a limit on acceptable displacement ductility in terms of demand for the retrofitted structure, are necessary design decisions that guide the proposed retrofit strategy. Application of the retrofit design through infills is demonstrated through example case studies.

Keywords: masonry infills; seismic assessment; retrofit; strengthening; soft-storey; performance based design; pushover analysis

1. Introduction

Failure in structures occurs when deformation demands exceed the deformation capacity of the affected elements. Older structures, designed prior to the introduction of modern detailing procedures are often marked by a number of adverse features such as small section columns, relatively stiff beams, inadequately confined joints and insufficient anchorage of longitudinal and transverse reinforcement. However, many such structures have survived major earthquakes, mostly because the deformation demands were controlled by significant lateral stiffness. The empirical recognition of

stiffness as a factor in mitigating localization of damage has been imprinted in the early versions of design codes worldwide. The first attempts for a structured seismic assessment procedure intended for reinforced concrete structures were supported on the concept that elastic stiffness of a building may be related to the area ratios of the vertical elements in the critical floor, including columns, walls and masonry infills [Fiorato *et al*., 1970]; in fact, there was such a successful correlation between the area ratio indices of vertical elements and the extent of reported damage in earthquake-struck urban centres that this parameter was used as a design guideline for new buildings, but also as rapid assessment parameter by field engineers. Recently, it was shown from basic mechanics that the seismic vulnerability of a given structure can be quantified by the distribution - in terms of area ratios in the floor plan - of the vertical elements, including both reinforced concrete members and masonry infills, ρ_c and ρ_{mw}, respectively [Thermou and Pantazopoulou, 2011]. Simple quantitative criteria have been derived utilizing fundamental principles of structural engineering, which link interstorey drift demand in the design earthquake to ρ_c and ρ_{mw} of the pilotis floor.

From a review of recent failures (Lefkas 2015 & 2013, Cephalonia 2014, Van 2011, L'Aquilla 2009, Achaia - Ilia 2008, Athens, Izmit & Düzce 1999, Aigio & Kozani 1995) it appears that from among the older reinforced concrete (R.C.) structures designed to previous generations of codes, the most vulnerable are buildings with stiffness discontinuities height-wise, such as pilotis and partially infilled frames with short column formations (Fig. 1). Deformation demands tend to localize in regions of reduced stiffness – such as the soft storey. Local failures occur because localized deformations (e.g. drift ratio demands) exceed the acceptance criteria (e.g. drift capacity) of the individual columns in the soft storey.

Figure 1. Pilotis-type multi-storey residential buildings, in Northern Greece.

A corollary to the findings cited above is, that geometric parameters, such as area ratios of load bearing elements, may be used beyond the needs of rapid seismic assessment [Pardalopoulos *et al*, 2013a, b], in order to guide fast retrofit designs. A simple idea is to set up a retrofit strategy as follows:

(a) limit the intensity of deformation demands by increasing the overall stiffness of the building at a relatively low cost, or,

(b) engage more storeys in deformation, by engineering the difference in stiffness between successive floors, so that a better distribution of deformation demands may be achieved throughout the structure.

In the Mediterranean region, where seismic activity is intensive and pilotis-type R.C. structures is a common practice, inexpensive retrofits in the form of post-installed infills in the soft-storey is a favoured practice. This type of stiffness increase, provided it is carried out properly, is very moderate, as compared to what could be achieved through R.C. infills; an advantage is that masonry infills are low-budget, versatile solutions. In most cases of pilotis buildings, the deficiency in first floor stiffness as compared to the upper floors is exactly due to the absence of infills in the first floor. For example in residential buildings, infills are placed immediately after construction of the reinforced concrete frame in the upper floors to create apartment walls, whereas the first floor is often left open for parking. By post-installing masonry infills in the first floor this deficiency between successive floors is

eliminated. This retrofit approach offers the advantage of reversibility (while not being necessarily invasive), whereas it moderates the magnitude of forces transferred to the foundation resulting from the stiffness enhancement and the increase of the foundation lever arm with respect to single column, or R.C. wall foundation. In this way, excessive foundation retrofit may not even be necessary – a situation that cannot be avoided with other more thorough interventions, such as R.C. jacketing and/or addition of R.C. walls – especially if these interventions are detailed according with capacity design principles (i.e. overdesigned foundations needed to support flexural yielding at the critical sections of jacketed columns and added R.C. walls).

Apart from the attractive arguments for it, post-installation of masonry infills has also received a lot of criticism in earthquake engineering practice and a few lingering issues need to be resolved before the method may be accepted as a legitimate engineering intervention in established retrofit design codes. These are related to the uncertainties necessarily associated with the masonry infill panel's resistance curve, its robustness and dependable ductility. Uncertainties also concern the degree of fixity, or contact, at the perimeter supports, which critically control the engagement of the infill walls during lateral displacement. (Perimeter masonry walls are only effective if they are in good contact with the perimeter frame, if they are built with cross-ties, rather than with independent wythes, in order to limit the slenderness of the diagonal compression strut that forms in the infill as it distorts in its own plane and also, if the mortar and blocks have compatible strengths). Infills have been blamed for causing damage to the adjacent columns [Stavridis et. al, 2012] – this is particularly the case if window openings in the infills cause short column behaviour. Based on the experimental evidence infill-induced column shear cracking has been reported to occur at drift levels well beyond 1%. However, even in these cases the

infilled frame was shown to sustain its strength to much higher levels of drift without collapse [Negro and Verzeletti, 1996; Mehrabi *et al*., 1996; Murty and Jain, 2000; Calvi and Bolognini, 2001; Varum, 2003; Serrato and Saatcioglu, 2004; Yeh and Liao, 2005; Kakaletsis and Karayannis, 2007; Hashemi and Mosalam, 2007;; Pujol *et al*., 2008; Korkmaz *et al*., 2010; Sigmund and Penava, 2013; Ozkaynak *et al*., 2014; Verderame *et al*., 2016; Su *et al*., 2016; Huang *et al*., 2016;]. Equally important is the integrity of the infill in out-of-plane action; here, tight-fit with the perimeter frame is again critical in order to secure some degree of boundary restraint to the infill against rocking, in response to ground shaking orthogonal to the wall's plane. Although inspired from the outstanding seismic performance of confined masonry (Fig. 2(a)), which in numerous earthquake cases prevented from collapse buildings with substandard construction details in their R.C. structural system, it is clear that post-installed masonry infills (Fig. 2(b)) are not nearly as effective. Evidently, the ideal contact is only secured by casting the R.C. frame on top and to the side of the confined walls. Therefore, to be effective, a retrofit scheme that uses masonry-infills should emulate as nearly as possible this method of construction [Chourasia *et al*., 2016; Matosevic *et al*., 2015; Perez Gavilan *et al*., 2015].

Figure 2. (a) Construction of a confined masonry building (available from https://cementtrust.wordpress.com/blog/page/21/); (b) post-installation of unconfined masonry infills in a contemporary new building with R.C. structural system.

Nevertheless, review of recent post-quake building performances shows that despite their brittleness and despite their enduring significant damage, infills can successfully mitigate the occurrence of catastrophic damage by diverting localization of demands away from the vulnerable regions of the building [Hossein and Kabeyasawa, 2004; Li *et al*., 2008; Haldar *et al*., 2013; Bolea, 2016;]. An example of the tendency for localization in the absence of infills is depicted in Fig. 3. To this end, the paper presents a practical retrofit design methodology, which is summarized for the sake of expediency, in the form of practical design charts. Using these charts, dimensioning and detailing of masonry infills in existing R.C. structures is controlled by target distributions of interstorey drift demand to a level below 0.5% (this drift level secures the elastic member response of the R.C. structural system), and a target estimate of the fundamental period as required by the designer. These decisions are in the designers' prerogative, but the use of the charts illustrate in an immediate manner the implications of these choices on the retrofitted response.

Figure 3. Soft-storey formation in 2-storey frame buildings at (a) Didahaika, Peloponnese (M6.5R Andravida Earthquake 2008) and (b.1,2) Livadi, Cephalonia (M6.1R Cephalonia Earthquake 2014), in Greece (available from www.itsak.gr).

2. Seismic rehabilitation of R.C. frame buildings with masonry infills

The beneficial effect of masonry infills, especially in the case of old substandard construction with no seismic detailing, has been demonstrated repeatedly in earthquake events and laboratory studies [Hashemi & Mosalam, 2006; Kyriakides and Billington, 2014; Misir *et al*., 2016]. In Greece, thousands of pre-1980s buildings,

which were poorly reinforced (hereafter referred to as substandard), survived the Athens 1999 earthquake with little or no damage, owing to the first storey infills. This was also the case in the 1978 earthquake in the city of Thessaloniki, where the number of collapses was surprisingly small considering the poor detailing in the multi-storey buildings of that period. Similar is the observation in many other reconnaissance reports from around the world [Mostafaei and Kabeyasawa 2004; Murti and Jain 2000]. The contribution of masonry infills to the lateral resistance of the structural system depends on the degree of engagement of the masonry to the vertical and horizontal components of the bay frame response.

Earthquake-resistant confined masonry stands as a discrete category, where masonry walls are the main load bearing elements expected to resist both gravity and lateral loads [Brzev, 2007]. In this type of construction, masonry walls are built first and subsequently the confining elements (tie-columns and tie-beams), which are much smaller in size than regular reinforced concrete columns and beams, are cast in place, encasing the pre-constructed masonry walls (Fig. 4(a, b)); a distinct advantage here is the interlocking of the cast-in-situ column with the edges of the masonry wall. But in the case of R.C. frame construction, R.C. columns and beams are the primary load-bearing elements, whereas masonry infills are built at a later stage. Thus, the degree of engagement between masonry and the surrounding frame is limited at best, or negligible. When the masonry walls are not monolithically connected with the frame members, but thin gaps, partially filled with mortar, exist between the infills and the surrounding frame, that weaken the interaction, they may be considered as non-structural components and their contribution to the lateral resistance of the building could be ignored in the interest of conservatism. However, there are construction techniques (e.g. R.C. laces or chainages (*Fr.*), shear connectors, wedged

bricks in the top layer) that improve integration between the infill walls and the surrounding load carrying components (Fig. 4(c)). In that case, a certain degree of connection with the surrounding structural elements is provided and thus, in these cases, infill walls are considered to contribute to the lateral load resistance of the buildings.

An outline of the mechanics of infill engagement during lateral in-plane and out-of-plane action are illustrated in Fig. 5, which underscores the need for some of the essential requirements during their construction. When distorted into in-plane shear action to accommodate the lateral drift of the surrounding frame, the infill panel develops principal strain directions that are approximately oriented along the two diagonals – so that a diagonal compressive strut provides the infill's resistance and the contribution thereof to the storey stiffness and strength (Fig. 5(a)). If the infill is robustly connected along its perimeter, it will elongate along the other diagonal through the formation of cracks parallel to the compressive load, otherwise it will simply debond at the corners, accelerating failure of the compressive strut. Openings that may interrupt, or even completely cancel the path of the compressive forces, may completely diminish the significance of the infill (Fig. 5(c)).
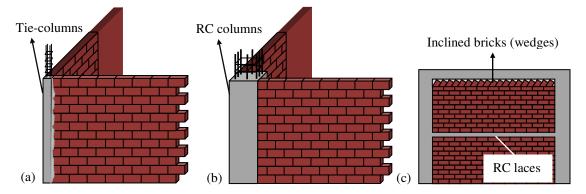

Figure 4. (a) Confined masonry; (b) Non-engineered masonry infills; (c) Construction techniques that strengthen the connection of the masonry infills to the surrounding structural elements emulating the confined masonry type of construction.

Examining the in-plane and out-of-plane stability of the diagonal compression strut it is worth noting that out-of-plane stability is controlled by the slenderness ratio, λ_s, which is obtained as the ratio of the bay diagonal, D, and the thickness of the wall, t: $\lambda_s = D/t$. An upper limit of 25 is set for λ_s to avoid premature out-of-plane buckling before crushing (EN; this is satisfied for a bay width of up to 4.5 m in usual 3.0 m high storeys, provided that the wall thickness is over 200 mm. Walls comprising 100 mm thick wythes that sandwich a layer of insulation material will buckle out of plane before crushing for much smaller span widths (Fig. 6). Monolithic connection of the infill with the perimeter structural frame will also increase the strut width that carries the compression force, thereby moderating the magnitude of stresses developed; poor perimeter connection would mean that force transfer is much more localized and therefore likely to expedite masonry failure.
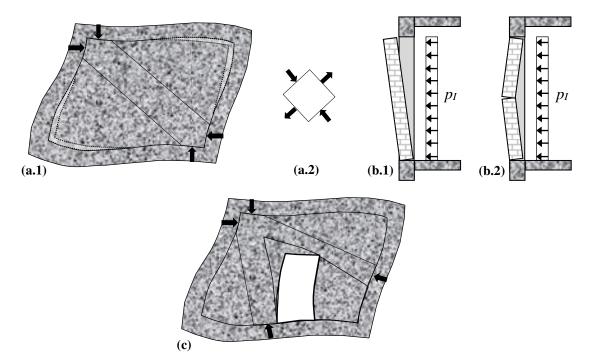

Figure 5. (a.1) In-plane distortion of masonry infill panel due to the lateral deformation of the surrounding R.C. frame; (a.2) Principal strain directions developing along the diagonal compressive strut of the infill panel; (b.1, 2) Failure modes of infill panels due to out-of-plane earthquake action; (c) Interruption of the path of the compressive forces by openings at the infill panel.

Figure 6. Failure of double-layer masonry infills during the 1999 Athens earthquake (available from http://katohika.gr/gn-blog/16-xronia-apo-to-sismo-tis-parnithas/)

Out-of-plane action of the infill may occur when the direction of the earthquake action is orthogonal to the plane of the infilled frame as depicted in Fig. 5(b). Here the infill develops inertia pressures equal to $p_I = w_m \cdot t \cdot (L^*/M^*) \cdot S_a$, where w_m is the specific weight (per unit volume) of masonry, L^* and M^* are the modal excitation factor and the equivalent translational modal mass of the Equivalent Single Degree of Freedom (ESDOF) idealization of the fundamental mode (Eq. 1) and S_a is the response acceleration of the building (if the earthquake hazard is given in spectral format, then S_a is the spectral response pseudo-acceleration that corresponds to the building's fundamental period). These pressures tend to overturn the infill if unsupported at the top and sides (Fig. 5(b.1)); if there is support reaction at the boundaries, the infill will be able to develop much higher resistance to overturning pressure (Fig. 5(b.2)) –this is another reason why it is important that if post-installed, infills must fit tightly with the perimeter frame.

2.1 Review of EC8 specifications for consideration of masonry infills

EC8 – Part 1 [EN 1998-1, 2004] (§4.3.6.1(1)) defines specifically the conditions that ought to be fulfilled by non-engineered masonry infills. Thus, they should be constructed after the hardening of the concrete frames, be in contact with the perimeter frame but without structural connection to it and be considered in principle as non-structural elements. Moreover, EC8 – Part 1 [EN 1998-1, 2004] (§4.3.6.1(5))

mentions that if engineered masonry infills constitute part of the seismic resistant structural system (implying that structural connection is provided between the masonry and the surrounding frame members), analysis and design should be carried out in accordance with the criteria and rules given for confined masonry. The contribution of masonry infill walls seems to be more pronounced in the case of frame buildings designed for a high ductility class, where the intrinsic lateral force stiffness and strength of the building are low, whereas the ductility and deformation capacity are high [Fardis *et al*., 2005]; in such a case, however, it is expected that the infills will fail before the frame structure attains its own ductility capacity at or beyond the "Significant Damage" performance limit, Eurocode 8 – Part 3 [EN 1998-3, 2005]; in this context infills are actually sacrificial elements in the structure (they are expected to fail in a severe earthquake and be replaced during repair. Their intended role is to deliver the building from pancake type collapse.) If the masonry infills are non-slender wythes, but have robustness through their thickness, then they should be explicitly included in the model for the seismic analysis of the building. Furthermore, it is recommended to consider any irregularity in plan and elevation, as well as the possible adverse local effects due to the frame-infill-interaction [EN 1998-1, 2004]. Another aspect that needs to be considered in detail is the high uncertainty related to the mechanical properties, the degree of attachment to the surrounding frame and the non-uniform degree of damage suffered during the earthquake. Last, but not least, is the influence of the shape, size and location of the openings in the axial stiffness and strength capacity of the masonry walls. EC8 - Part 1 [EN 1998-1, 2004] mentions that strongly irregular, unsymmetrical, or non-uniform arrangements of infills in plan should be avoided. Spatial models should be used for the analysis of the structure in the case of severe irregularities in plan due to the unsymmetrical arrangement of the

infills. The Greek Code for Structural Interventions, [GRECO, 2013] provides some practical rules on how to model the masonry infills in lateral load analysis of building structural systems, including consideration of any openings.

2.2 Function of infills as a retrofit scheme

Frame structures, particularly of older construction, feature relatively lightly reinforced columns and heavy floor diaphragms, dictated by working stress design, which was used in past engineering practice for structural dimensioning and detailing. Structures of this type are commonly referred to as shear-type buildings, because most of the relative floor displacement during lateral sway would occur in the lower floors. The fundamental mode of vibration in these structures engages a very large fraction of the total mass (more than 75%) and as such, it is sufficient in most cases to use an Equivalent Single Degree of Freedom (ESDOF) idealization in the first mode in order to assess performance of the structure from the acceleration/displacement spectra of the design earthquake hazard. In deriving the work-equivalent dynamic properties of the ESDOF that represents the structure, the following expressions are generally used:

$$\text{Equivalent translational Mass, } M^*: \quad M^* = \sum_{i=1}^{n} m_i \cdot \Phi_i^2 \qquad (1a)$$

$$\text{Modal excitation factor, } L^*: \quad L^* = \sum_{i=1}^{n} m_i \cdot \Phi_i \qquad (1b)$$

$$\text{Equivalent translational Stiffness } K^*: \quad K^* = \sum_{i=1}^{n} k_i \cdot \Delta\Phi_i^2 \qquad (1c)$$

Parameter $\Delta\Phi_i$ in the above expressions is the displacement difference of successive floors in the normalized fundamental mode. Due to the square power of $\Delta\Phi_i$ in K^*, equivalent stiffness is dominated by the stiffness contributions of the most compliant parts of the structure. In the case of a soft storey the most compliant floor is the pilotis

floor and thus K^* is nearly equal to the lateral stiffness of the pilotis floor. By increasing the relative magnitude of the pilotis stiffness, a better distribution of $\Delta\Phi_i$ is achieved as shown in Fig. 7 – Illustrative examples are shown in Figs. 16-18.
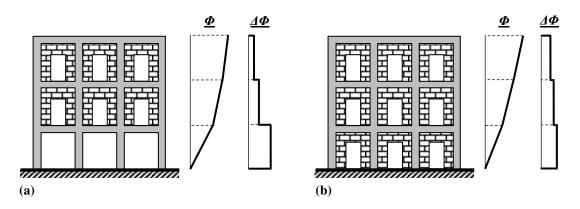

Figure 7. Improvement of the $\Delta\Phi$ distribution of a pilotis-type building (a) by adding masonry infill panels in the building's first storey (b)

3. Lateral stiffness of the structure

The lateral stiffness of a frame building with rigid diaphragms comprises the sum of the work equivalent contributions of the individual storey stiffnesses. In turn, the individual storey stiffness results from the summation of the lateral stiffness of the storey's vertical members, i.e., columns and masonry infill walls [Thermou and Pantazopoulou, 2011].

- *Reinforced concrete columns*: Assuming cracked stiffness values, the storey stiffness contribution owing to a total of ℓ_c number of R.C. columns in a single floor is equal to:

$$K_{c,i} = \sum_{j=1}^{\ell_c} k_j^c \approx \frac{A_f}{\alpha \cdot h_{cl,i}} \cdot E_c \cdot \left(\frac{h_{c,ave}}{h_{cl,i}}\right)^2 \cdot \rho_{c,i} = \frac{A_f}{h_{cl,i}} \cdot D^c \cdot \rho_{c,i} \text{ , where } D^c = \frac{E_c}{\alpha} \cdot \left(\frac{h_{c,ave}}{h_{cl,i}}\right)^2 \quad (2)$$

and, E_c is the elastic modulus of concrete, α accounts for the effective reduction of concrete stiffness in the columns due to cracking (=2 for very low levels of lateral

drift ratio, or =3 for drift ratios in the order of 0.5%), $h_{c,ave}$ is the average height of the R.C. column cross sections in the sway direction considered, $h_{cl,i}$ is the clear height of the storey and $\rho_{c,i}$ is the column's area ratio in the floor plan at i-th storey, i.e., $\rho_{c,i} = A_c / A_f$ (A_f is the typical floor area and A_c the total column area).

- *Infill masonry walls*: The translational stiffness of an infill masonry wall deforming in its plane is estimated with reference to a diagonal strut used to idealize the infills' function as a stiffening link (see Fig. 8(a)). The stiffness value is a secant measure, obtained from the ratio of the wall's estimated lateral load strength to the corresponding storey distortion. The applied lateral force is equal to the horizontal component of the strut and may be estimated from the following expression according with EC8 – Part 1, [EN 1998-1, 2004] and EC8 – Part 3, [EN 1998-3, 2005]:

$$V_{\max,j} = N_j \cdot \cos\alpha = \left(0.10 \cdot A_{mw,j} \cdot f_{mw,j} \right) \cdot \cos\alpha \; ; \; \cos\alpha = \frac{\ell_{mw,j}}{L_j} \; ; \; L_j = \sqrt{\ell_{mw,j}^2 + h_{cl,i}^2} \quad (3)$$

In Eq. 3 $V_{max,j}$ is obtained from the product of the compressive strength of the masonry, $f_{mw,j}$, multiplied by the effective area of the strut. This is taken equal to 10% of the wall plan area in its plane of action, $A_{mw,j}$. Term $\ell_{mw,j}$ is the masonry wall length and $h_{cl,j}$ is the clear storey height. Storey distortion is given by the interstorey lateral displacement, $\theta_i \cdot h_i$. Storey drift, θ_i, is expressed as a multiple of the infill wall's notional yield distortion, θ_y^{mw}, through the level of ductility attained by the infill wall when the surrounding R.C. frame reaches its own yielding drift limit, $\theta_{i,y}$. This ductility index is denoted here by parameter μ_y^{mw}. Thus, the secant stiffness of the j-th masonry pier oriented parallel to the direction of the earthquake action and contributing to the floor translational stiffness at the onset of yielding of the perimeter concrete frame is,

$$k_{y,j}^{mw} = \frac{V_{max,j}}{\theta_y^{mw} \cdot \mu_y^{mw} \cdot h_i} = \frac{A_f}{h_i} \cdot \frac{0.10 \cdot f_{mw,j}}{\mu_{y,j}^{mw} \cdot \theta_{y,j}^{mw} \cdot \sqrt{1 + h_{cl,i}^2 / \ell_{mw,j}^2}} \cdot \rho_{mw,j} = \frac{A_f}{h_i} \cdot D_j^{mw} \cdot \rho_{mw,j} \qquad (4)$$

where, A_f is the floor area of the critical storey, h_i is the storey height, $f_{mw,j}$ is the compressive strength of the j-th masonry pier, $\rho_{mw,j}$ is the dimensionless area of masonry infill walls at i-th storey (i.e., $\rho_{mw,j} = A_{mw,j}/A_f$), $\theta_{y,j}^{mw}$ is the drift ratio at yielding of the infill wall and $\mu_{y,j}^{mw}$ is the level of ductility attained by the infill wall at the point of yielding of the surrounding R.C. frame, i.e., $\mu_{y,j}^{mw} = \theta_{i,y}/\theta_y^{mw}$. The rotation of a masonry wall at apparent yielding (abrupt change of stiffness) is taken equal to 0.2% [Karantoni *et al.*, 2016].

As illustrated in Fig. 8(b) the secant stiffness of wall infills decays beyond the value given by Eq. 4, with increasing magnitude of the imposed drift demand. The wall's distortion capacity at notional "yield" (i.e., at the point where a sharp change of stiffness is observed in the resistance curve of the masonry infill, see Fig. 8(b)) and the corresponding ultimate value may be defined according to GRECO [2013] by the following set of equations:

$$\theta_{y,j}^{mw} = \gamma_{y,j}^{mw} = \left(\frac{\ell_{mw,j}}{h_{cl,i}} + \frac{h_{cl,i}}{\ell_{mw,j}} \right) \cdot (1.0 \div 1.5) \cdot 10^{-3} \qquad (5a)$$

$$\theta_{u,j}^{mw} = \gamma_{u,j}^{mw} = \left(\frac{\ell_{mw,j}}{h_{cl,j}} + \frac{h_{cl,j}}{\ell_{mw,j}} \right) \cdot (2.0 \div 3.5) \cdot 10^{-3} \qquad (5b)$$

where $\ell_{mw,j}$ is the masonry infill's length and $h_{cl,j}$ is the clear storey height.
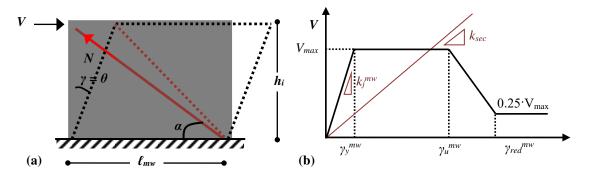
Figure 8. (a) Behavioral model of the infill masonry wall in tis plane of action; (b) Resistance curve for masonry pier element suggested by GRECO [2013].

- *Typical storey of the building*: Considering that the i-th typical storey of the building comprises both R.C. columns and infill masonry walls, the contribution of both types of vertical members can be represented by the composite area ratio, ρ_i:

$$\rho_i = \rho_{c,i} + \frac{D^{mw}}{D^c} \cdot \rho_{mw,i} \; ; \; D^c = \frac{E_c}{\alpha} \cdot \left(\frac{h_{c,ave}}{h_{cl,i}} \right)^2 , \; D^{mw} = \frac{0.1 f_{mw}}{\mu_y^{mw} \cdot \theta_y^{mw} \cdot \sqrt{1 + \frac{h_{cl,i}^2}{\ell_{mw}^2}}} \qquad (6)$$

Therefore, the total stiffness K_i of the i-th typical storey is estimated from:

$$K_i = \sum_{j=1}^{\ell_c} k_j^c + \sum_{j=1}^{\ell_{mw}} k_{y,j}^{mw} = \frac{A_f}{h_i} \cdot \left(D^c \cdot \rho_{c,i} + D^{mw} \cdot \rho_i^{mw} \right) = \frac{A_f}{h_i} \cdot D^c \cdot \rho_i \qquad (7)$$

4. Interstorey drift envelopes for retrofitting with masonry infill walls

Retrofit design of substandard R.C. structures is based on the systematic correction of the buildings' deflected shape at the instant of their maximum seismic response, so as to achieve a near-uniform distribution of interstorey drift demand. Through this process, concentration of anticipated damage at certain locations of the vibrating structure (i.e. soft-storey formation) may be avoided, by increasing the translational stiffness of the corresponding storey through the addition of new structural elements or strengthening of the existing ones.

The Interstorey Drift Spectra (IDS) representation is a practical design tool that facilitates direct insight into the relationships between drift demand and the required stiffness under lateral sway of the building. It was developed by Thermou and Pantazopoulou [2011] and may used both for assessment [Pardalopoulos *et al.*, 2013a, b] and rehabilitation of existing buildings [Thermou *et al.*, 2012a, b].

The elastic value of the *i*-th storey interstorey drift, ID_i, is given by:

$$ID_i = \frac{(\Phi_i - \Phi_{i-1})}{h_i} \cdot \Delta_i = \frac{\Delta\Phi_i}{h_i} \cdot \frac{L^*}{M^*} \cdot S_d \tag{8}$$

where, $\Delta\Phi_i$ is the difference in the lateral response shape between two successive storeys, h_i is the storey height, S_d is the spectral displacement of the equivalent SDOF system. For any chosen target response shape, Φ, the values of L^* and M^* are calculated from the storey masses, m_i, as defined in Eqs. 1(a), (b).

Considering that nonlinear behavior of the retrofit is often controlled by the existing reinforcement anchorages, which may remain a weak zone of behavior even after rehabilitation, it is generally advisable that the ductility demand targeted for the structural system should not exceed the value of 2.5 [Pantazopoulou et al. 2016]. Once the likelihood of localization has been eliminated through proper selection of the target response shape, and in order to re-engineer the structure through retrofit, the individual target member rotation demand that would be consistent with the target ductility demand may be estimated from:

$$\text{For Columns: } ID_{y,i}^c = \lambda_c \cdot \frac{\Delta\Phi_i}{h_i} \cdot \frac{L^*}{M^*} \cdot \frac{S_d}{q} \tag{9a}$$

$$\text{For Beams: } ID_{y,i}^b = \lambda_b \cdot \frac{\Delta\Phi_i}{h_i} \cdot \frac{L^*}{M^*} \cdot \frac{S_d}{q} \tag{9b}$$

where q is the system behavior factor that corresponds to the targeted system ductility selected in the retrofit (the value of q may be calculated from pertinent q-μ-T relationships; one such example is, $q = (\mu+1)/2$ for $T \geq T_C$ and $q = 1+(\mu-1)\cdot(T/(2\cdot T_C))$ for $T < T_C$ [EN 1998-1, 2004]. Coefficients λ_c and λ_b distribute the frame joint rotation of the ith floor, θ_i, to members that converge in each joint (to beams and columns) according to the individual member stiffness: $\theta_{c,i}=\lambda_c\cdot\theta_i$, and $\theta_{b,i}=\lambda_b\cdot\theta_i$, where $\lambda_c = \lambda / (1 + \lambda)$, $\lambda_b = 1 / (1 + \lambda) = 1 - \lambda_c$ with λ equal to:

$$\lambda = \frac{n_b \cdot E \cdot I_b \cdot h_i}{n_c \cdot E \cdot I_c \cdot L_b} \tag{10}$$

where n_b and n_c represent the numbers of beams and columns that converge to a typical floor joint, $E\cdot I_b$ and $E\cdot I_c$ are the secant to yield sectional stiffnesses of beams and columns, h_i is the storey height and L_b is the beam span. In cases of older construction, where beams were typically much stiffer than the columns due to serviceability requirements, it is justified to take the ratio λ_c equal to 1, which means that all the deformation is mostly taken by the columns. (This assumption is prerequisite for the validity of Eq. 1(c) which only accounts for the work done in the columns; if retrofit alters this stiffness ratio, e.g. through jacketing of the columns, then the corresponding work equivalent stiffness contributed to the floor through deformation of the beams would have to be included in Eq. 1(c) [Thermou and Pantazopoulou, 2011].

The type I elastic spectrum of EN 1998-1 [2004] is used to define the design seismic hazard. The spectral displacement demand for a design region 0.15 s $< T <$ 2.00 s, and for a moderate stiffness subsoil of class B with $S = 1.20$, $\beta_0 = 2.50$, $T_B = 0.15$ s, $T_C = 0.50$ s, $q = 1.00$ is defined as follows:

-For 0.15s $\leq T \leq$ 0.50s:

$$S_e(T) = a_g \cdot S \cdot \eta \cdot 2.5 \xrightarrow{S=1.2,\eta=1} S_e(T) = 3 \cdot a_g \;\; ; \;\; S_d(T) = S_e(T) \cdot \left(\frac{T}{2 \cdot \pi}\right)^2 \Rightarrow$$

$$S_d(T) = 0.076 \cdot a_g \cdot T^2 \tag{11a}$$

-For 0.50s $< T \leq$ 2.00s:

$$S_e(T) = a_g \cdot S \cdot \eta \cdot 2.5 \cdot \frac{T_C}{T} \xrightarrow[T_C=0.5s]{S=1.2,\eta=1} S_e(T) = 1.5 \cdot a_g / T \; ; \;\; S_d(T) = S_e(T) \cdot \left(\frac{T}{2 \cdot \pi}\right)^2 \Rightarrow$$

$$S_d(T) = 0.038 \cdot a_g \cdot T \tag{11b}$$

In Eq. 11 a_g is the peak ground acceleration (PGA) and T is the period of an n-storey building. In case of constant storey plan geometry along the height of the building and a translational storey stiffness distribution such as to produce the shear response shape, it has been shown that the period T may be approximated from [Thermou and Pantazopoulou 2011]:

$$T = 2 \cdot \pi \cdot \sqrt{\frac{M^*}{K^*}} = A \cdot \sqrt{\frac{m}{K_1}} = A \cdot Q = 1.76 \cdot (2.25 \cdot n + 1) \cdot Q \tag{12}$$

where, m is the storey typical mass and K_1 is the cracked-sections lateral stiffness of first storey. A is a parameter that takes into account the type of the lateral response shape and is related to the number of stories n as given in Eq. (12). The term Q is obtained from:

$$Q = \left(\frac{m}{K_1}\right)^{0.5} = \left(\frac{\gamma \cdot h_i}{D^c \cdot \rho_1}\right)^{0.5} \tag{13}$$

where the storey mass has been substituted by $m = \gamma \cdot A_{fl}$ with γ the average mass per unit area of the floor, D^c is the stiffness coefficient of the first storey ($K_1 = A_{fl} \cdot D^c \cdot \rho_1 / h_1$, see Eq. (6) for further detail), and ρ_1 is the composite area ratio of the vertical members of the first storey (see Eq. (6)).

After algebraic manipulation of the above expressions and assuming that the critical storey is the first storey, drift demand in the first floor of the structure, ID_1, is related to the composite area ratio of the vertical floor members, ρ_1. Derivations are based on the assumption that the fundamental shape of lateral vibration may be approximated by a shear response shape according with:

$$\Phi(z_i) = \sin\left(\frac{\pi \cdot z_i}{2 \cdot H}\right) \tag{14}$$

Using this definition, the seismic demand (expressed in terms of storey drift in the i-th floor) may be quantified from Eq. 8, after algebraic manipulations according with:

$$0.15 \leq T \leq 0.50: \quad ID_1 = 0.235 \cdot a_g \cdot (2.25 \cdot n + 1)^2 \cdot \Delta\Phi_i \cdot \frac{\Phi_s}{h_i} \cdot \frac{m}{K_1} \tag{15a}$$

$$0.50 < T \leq 2.00: \quad ID_1 = 0.067 \cdot a_g \cdot (2.25 \cdot n + 1) \cdot \Delta\Phi_i \cdot \frac{\Phi_s}{h_i} \cdot \left(\frac{m}{K_1}\right)^{0.5} \tag{15b}$$

where, n is the number of stories. The term (m/K_1) equals to Q^2, as this is defined in Eq. 13. Parameter Φ_s corresponding to the shear response profile is calculated in Table 1 from the following expression (Φ_i is the value of the shape function in the i-th storey):

$$\Phi_s = \sum_{i=1}^{n} \Phi_i \left/ \sum_{t=1}^{n} \Phi_i^2 \right. \tag{16}$$

Table 1. Values of coefficient Φ_s for shear-type buildings with 2 to 8 storeys, at the instant of maximum seismic response.

	Number of storeys						
	2	3	4	5	6	7	8
Φ_s	1.138	1.183	1.205	1.219	1.228	1.234	1.239

4.1 Design charts for various retrofit scenarios

From the above derivations, two alternative types of design charts may be derived as depicted in Figs. 9 and 10. The graphs in Fig. 9 relate the interstorey drift demand of the 1st storey, ID_1, to the composite area ratio of the vertical floor members of the first storey (i.e. columns and masonry walls), ρ_1, whereas the graphs in Fig. 10 present the various combinations between $\rho_{c,1}$ and $\rho_{mw,1}$ for values of target interstorey drift, ID_1, ranging between 0.1 and 0.3% ($0.5 \leq \mu_y^{mw} \leq 1.5$) and a specific number of floors (Fig. 10 was drawn for $n = 2$). The selected PGA value in Figs. 9 and 10 correspond to the three seismicity zones in Greece (Zone 1: 0.16g, Zone 2: 0.24g, Zone 3: 0.36g). The expression for determining the interstorey drift demand is modified depending on the period range (see Eq. 15(a) and Eq. 15(b)). The curves of Figs. 9 and 10 were derived assuming a common concrete grade C12/15 (f_{ck} =12 MPa), which corresponds to B160, commonly used in the era of construction. Also assumed was a mass per unit area of the floor, $\gamma = 1$ t/m^2 and a compressive strength of the masonry $f_{mw} = 4$ MPa. The storey and columns' height, h_i and $h_{cl,i}$, were taken equal to 3.2 and 2.7 m. The average length of the masonry walls was $\ell_{mw,ave} = 3.0$ m, whereas the column cross section height was determined by the following rule: $h_{c,ave} = 0.30 + (n-2) \cdot 0.05$ for $2 \leq n \leq 4$ (n is the number of storeys). For $n > 4$ the column cross section height was taken equal to 0.50 m. For a different value of mass per unit area, γ, the ID_1 should be multiplied by this value (without the units) if $T \leq 0.5$s, of by $\sqrt{\gamma}$ if $T > 0.5$s.
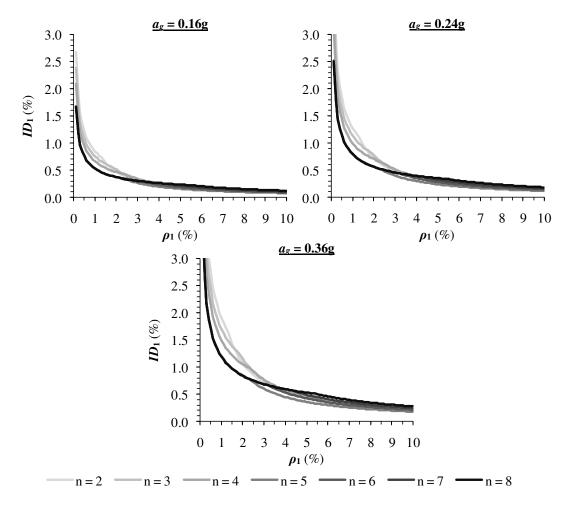
Figure 9. Design charts that relate the required composite floor area ratio of vertical members to the interstorey drift demand ratio for a mass per unit area of the floor, $\gamma = 1.0 \ t/m^2$, for $a_g = 0.16$, 0.24 and 0.36g, obtained assuming that column dimensions in the critical floor increase with the number of storeys, for buildings that are shorter than 4 storeys, but assuming constant column dimensions for taller structures
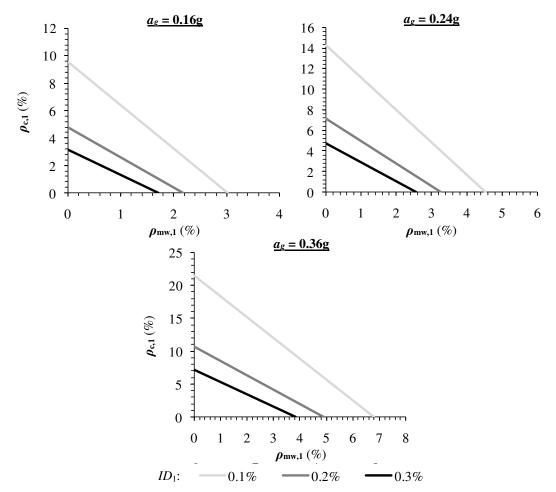
Figure 10. Design charts that relate the various combinations between $\rho_{c,1}$ and $\rho_{mw,1}$ for target interstorey drift values ranging between 0.1 and 0.3%, for $n = 2$, $\gamma = 1.0$ t/m^2 and $a_g = 0.16$, 0.24 and 0.36g.

The design charts presented in Figs. 9 and 10 may be used either for assessment of an existing frame building, or for determining the retrofit scenario. In the latter case, for a 2-storey building subjected to a PGA = 0.16g, if the demand in terms of interstorey drift of the first storey is to be limited by $ID_1 = 0.3$ % (which is very low, corresponding only to cracking of the masonry walls), then, the required composite floor area ratio of the vertical members would be $\rho_1 = 3.2$ % (Fig. 9). For the scenario where the existing column's area ratio is $\rho_{c,1} = 1.2$ %, then the required masonry infill walls' area ratio is $\rho_{mw,1} = 2.6$ %. In case of assessment, the existing composite floor area ratio of the vertical members, ρ_1, is evaluated; then, by utilizing the charts of Fig. 9, the drift demand, ID_1, is determined. This value is compared with

the nominal drift capacity at yielding for the existing building, $ID_{1,ex}$. If the estimated drift demand, ID_1, exceeds the limiting value, $ID_{1,ex}$, then some type of inelasticity is anticipated, provided that brittle failure modes of the vertical structural elements of the building are not expected to occur prior to their flexural yielding [Pardalopoulos *et al*., 2013a, b], otherwise the building survives.

4.2 Illustrative example

Application of the rapid retrofit design procedure developed in this paper is illustrated in this section through application to a residential, two-storey R.C. building in Didahaika, Western Peloponnesus, Greece (Fig. 11). The building was constructed in the early 1980's, having external dimensions in plan 12.80 by 14.20 m, whereas the heights of the first and the second storey were 4.00 and 3.50 m, respectively. The structural system was formed as an orthogonal grid of columns, beams and slabs, according to typical construction practice of R.C. frame structures in Southern Europe. All columns comprised a 300 by 300 mm square cross section, except of the first storey columns C5, C6, C7 and C8, whose cross section was 350 by 350 mm. Details of the column geometry and longitudinal reinforcement are presented in Table 2. Based on site reconnaissance evaluation, column stirrups were approximately $\varnothing6/200$ mm. Slab thickness was 140 mm in both storeys. All beams parallel to the *X* direction in plan were 200 mm (width) by 500 mm (height, including the slab thickness), whereas beams parallel to the *Y* direction in plan were 200 x 600 mm. Beams in the *X* direction had 4 $\varnothing12$ mm reinforcing bars running along their length both at top and at bottom, whereas beams in the *Y* direction had 4 $\varnothing14$ mm reinforcing bars at the top and an equal amount at the bottom of their cross section. The examined building had masonry infills only in its upper storey (red areas in Fig. 11a) which led to the formation of a soft first storey in the lower floor, during the

6.5R Magnitude 06-08-2008 Andravida earthquake (Fig. 11c) and consequently to the collapse of the entire structure (Fig. 11b). Based on tests conducted on material samples collected from the collapsed building, the concrete was classified as B160 (corresponding to contemporary concrete category C12/15 according to EN 1992-1-1 [2003]), while longitudinal reinforcement and stirrups were found to have smooth surface and were classified as St I (f_{yk} = 220 MPa, f_{uk} = 500 MPa). Failure of the building was due to shear failure of the floor-level columns due to the inadequate placement of stirrups (an estimated shear contribution by web reinforcement amounting to 12.7kN per column).
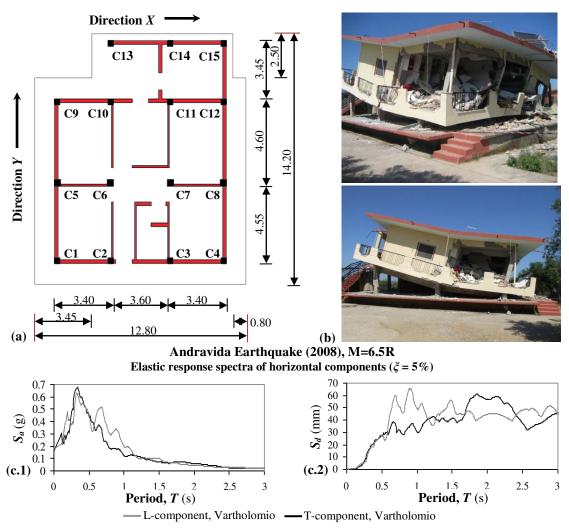

Figure 11. (a) Plan configuration of the 2nd floor of the house in Didahaika; (b) Photos of the collapsed building; (c.1, 2) Andravida (Pyrgos, Greece) Earthq. (8th June 2008), elastic response spectra (Total Acceleration & Relative Displacement) of horizontal components.

Table 2. Column dimensions and reinforcement of the collapsed house.

Storey	Columns	Section Dimensions (mm)	Long. Reinforcement (mm)	Stirrups (mm)
1st	C1 – C4, C9 – C15	300 × 300	4 ∅20	∅6 / 200
	C5 – C8	350 × 350	4 ∅20 + 4 ∅18	∅6 / 200
2nd	C1, C4, C9, C12	300 × 300	4 ∅20	∅6 / 200
	C2 – C3, C5 – C8, C10 – C11, C13 – C15	300 × 300	4 ∅16	∅6 / 200

Retrofit of such a structure to avoid collapse would have to follow one of two alternatives: (a) either to increase the deformation capacity of the soft storey columns to levels beyond the demand, through confinement (e.g. jacketing), or (b) to reduce the deformation demand so that collapse would be avoided, through stiffness increase in the soft storey (e.g. addition of infills). The second option is pursued here.

The design of the retrofit solution involving the addition of infills is a two step procedure:

- *Step 1: Determination of the required composite floor area ratio of vertical members*. First, determine the total required area of vertical structural elements in the soft storey of the building, ρ_1, using the design chart of Fig. 9 associated to the seismicity zone (expressed here by the zonal PGA) that corresponds to the building's site. If yielding of the longitudinal reinforcement would be the prevailing failure mechanism of the vertical R.C. members of the examined building, the limiting value of ID_1 used in the design charts of Fig. 9 can be taken equal to 0.5% as a rough estimate [Priestely *et al.*, 1996], which corresponds to flexural yielding of R.C. columns. However, in the case of the examined building, owing to the small size of its columns and their insufficient transverse reinforcement, application of the *Rapid Seismic Assessment Procedure* [Pardalopoulos *et al.*, 2013a, b] indicated that the value of ID_1 used in the calculations for determining ρ_1 in both *X* and *Y* plan directions would have to be limited to 0.2%, to avoid premature web shear failure in the columns. Therefore, considering that the

maximum value of ground acceleration expected at site of the examined building is a_g = 0.24g, the value of the required composite floor area ratio of vertical elements in each of the X and Y plan directions, $\rho_{1,X}$ and $\rho_{1,Y}$, would be 5.7% (Fig. 12(a)), calculated according to Table 3.

Table 3. Calculation procedure for the determination of ρ_1 based on the seismic demand.

ID_1 (%)	$S_d(T)$ (m)	T (s)	Q	γ (t/m^2)	D^c (kN/m^2)	ρ_1 (%)
0.20	0.010	0.236	0.024	0.75	89151	5.7

- *Step 2: Determination of the required floor area ratio of masonry infills.* The layout of the masonry infills needed to be added in the first storey of the examined building is the final stage of the retrofit design. Note that the only vertical structural elements that existed in this storey were the R.C. columns of the building ($\rho_{c,X} = \rho_{c,Y} = 1.23\%$). Thus, to fulfill the requirement of $\rho_{1,i}$ (i = X or Y), as this has been calculated in Step 1, the floor area ratio of masonry infills that needs to be added in each direction of the first storey of the examined building, $\rho_{mw,i}$, is estimated from Eq. (6) equal to 2.8% (Fig. 12(b)), according to the procedure presented in Table 4. A possible arrangement of the added masonry infills of 250 mm thickness is illustrated in Fig. 12(c).

Table 4. Determination of $\rho_{mw,1}$, based on the calculated ρ_1.

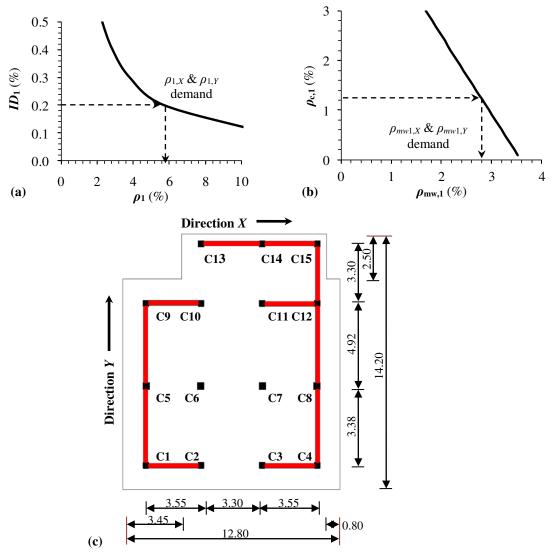| ρ_1 (%)	$\rho_{c,1}$ (%)	ℓ_{mw} (m)	f_{mw} (MPa)	D^m (kN/m^2)	D^c (kN/m^2)	$\rho_{mw,1}$ (%)
5.7	1.23	3.40	4.0	143456	89151	2.8

Figure 12. Design charts for the examined building based on the EN 1998-1 design spectrum applied at the site: (a) Relationships between the interstorey drift, ID_1 and the composite area ratio of the vertical floor members, ρ_1, for the 1st floor; (b) Relationships between $\rho_{c,1}$ and $\rho_{mw,1}$ for the interstorey drift at failure of the 1st storey; (c) Proposed arrangement of masonry infills layout at the 1st floor.

5. Analytical assessment of the effectiveness of masonry infills as a retrofit measure to mitigate localization of drift ratio

To assess the effectiveness of infills as a retrofitting strategy intended to control the interstorey drift demand height-wise in R.C. buildings non-conforming to modern requirements, simulation and analyses of such types of buildings were carried out. For this purpose, eight multi-storey, pilotis-type, R.C. buildings, representative of existing buildings built in Southern Europe up to the early 1980s with regards to configuration

of their structural system, were subjected to time-history dynamic analyses under a sequence of ground motion records representative of the seismicity of the region. Building dynamic response was compared to the seismic demand derived from application of the presented procedure obtained before and after the addition of infills at the first storey level.

5.1 Description of the building used in the analytical study

All of the examined buildings had a rectangular plan configuration, with structural system comprising of two 6.00 m bays o.c. (on column centers) in each principal direction (Fig. 13); typical floor height was 3.20 m. With regards to their structural system, in all buildings the beam sections were 0.60 m high by 0.25 m wide, whereas the monolithic slabs were 0.15 m thick and were assumed axially rigid for the purposes of the analyses. In all cases the column section external dimension orthogonal to the direction of sway (i.e. parallel to the Y axis in plan), $b_{c,Y}$, was 0.40 m. To investigate the influence of the parameter ρ_c in the seismic response of the examined R.C. buildings, three different groups of buildings were produced, by considering different external dimension in the column sections in the X direction of the plan, $b_{c,X}$. In this manner three building groups are created: in group A the typical column size is, $b_{c,X} = 0.25$ m ($\rho_c = 9 \cdot 0.25 \cdot 0.40/(12 \cdot 12) = 0.625\%$), in group B columns have a square cross section ($b_{c,X} = 0.40$ m, $\rho_c = 1.0\%$) and in building group C columns have typical dimension $b_{c,X} = 0.60$ m ($\rho_c = 1.5\%$). Additionally, all buildings where considered to have 150mm thick (this is a theoretical example, for the sake of illustration) masonry infills in all of their storeys, except of the first, spanning in the perimeter of the building, parallel to the seismic excitation. Time-history dynamic analyses were carried out on three- and a six-storey building belonging to group A and a three-, a six- and an eight-storey building belonging to each of groups

B and C. Materials considered in the analyses were also representative of the materials used in Southern Europe up to the early 1980s: C12/15 (f_{ck} = 12 MPa) for the concrete and StIII ($f_{s,yk}$ = 420 MPa) for the longitudinal reinforcing. Compressive strength of masonry infills, $f_{mw,j}$, was considered 4.0 MPa.
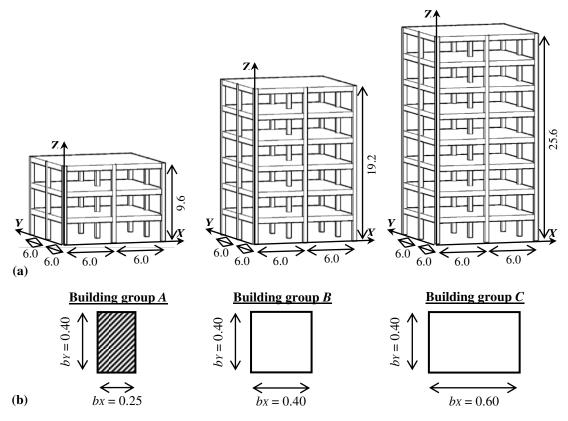

Figure 13. (a) Three-dimensional view of the R.C. structural system of the 3-, 6- and 8-storey buildings considered in the dynamic analysis (dimensions in m); (b) Cross sections of the columns used in the different building groups.

Dynamic analyses were carried out using the OpenSees 2.5.0 finite element analysis platform [OpenSees 2016]. As a point of reference the elastic response of the buildings was calculated. R.C. buildings of the type studied (smooth rectangular stirrups of 6–8 mm diameter and StI (f_{yk} = 220 MPa) spaced at 250–300 mm o.c. along the member lengths and anchored with 90° hooks in the ends, longitudinal reinforcement of StIII (f_{yk} = 420 MPa) at relatively low area ratios, concrete quality of Bn150 to Bn200 (f_{ck} = 12 to 16 MPa), unconfined lap-splices having starter bars with arbitrary lengths [*fib* Bulletin 24, 2003]) are expected to develop premature failure of

gravity load bearing elements (columns), prior to attainment of the nominal yielding displacement [Pardalopoulos *et al*., 2013a, b].

5.2 Modelling assumptions

Columns and beams were modeled as elastic elements (element *elasticBeamColumn*) with rigid links in the joint regions (Fig. 14). Concrete elastic modulus was considered as $E_c = 22.9$ GPa [Model Code 2010, 2010] Columns' sectional stiffness, $E_c \cdot I_{eff}$, was taken equal to 50% of the corresponding gross property, to account for member cracking [EN 1998-1, 2004]. Beams were modeled as T-shaped cross-sections with effective width equal to $b_w + 2 \cdot d_{beam}$ (b_w is the width and d_{beam} is the depth of the beam's web). To calculate beams' sectional stiffness, $E_c \cdot I_{eff}$, sectional response of fully cracked cross section was considered ($E_c \cdot I_{eff} = M_y / \varphi_y$), where, $M_y = \rho_{s1} \cdot 0.9 \cdot d \cdot f_y \cdot D_d$, where $d = 0.552$ m (effective depth of beams), D_d (diameter of longitudinal reinforcing bar of the beam) was assumed 14 mm, top and bottom longitudinal beam reinforcement ratios (ρ_{s1} in the expression of the flexural moment M_y above) were, 1% and 0.7%, respectively, $\varphi_y = 2.1 \cdot \varepsilon_y / h$ [Priestley *et al*., 1996], $\varepsilon_y = f_y / E_{steel}$ and $h = 0.60$ m. Due to the restrictions associated with the *elasticBeamColumn* F.E. linear elements of OpenSees [2016] in using a single value of $E_c \cdot I_{eff}$, the effective stiffness of beams was considered as the weighted average value considering the flexural moment diagram along the beams, equal to 35% of the corresponding gross property. Torsional stiffness for both columns and beams was taken equal to 10% of the corresponding gross property, accounting for sectional cracking. Masonry infills where simulated by using two diagonal linear truss elements (element *truss*) in each opening, operating only in compression, to connect the ends of the successive columns (Fig. 14). Equivalent sectional properties of the two truss

elements used in the simulation of each infill masonry wall were selected so that the lateral stiffness contribution of the wall, calculated according to Eq. (4), be equally mobilized regardless of the direction of sway. Gravity design loads included apart from self weight, a uniform distributed load of 1.00 kN/m^2 and a linear load of 5.6 kN/m on beams to account for infill walls. A uniformly distributed live load of 2.00 kN/m^2 was also considered. Mass was assumed lumped at the center of mass *(CM)* of each individual structural member, whereas viscous damping was taken equal to 5% of critical damping (modeled using the Rayleigh damping coefficients *a* and *b* [Clough and Penzien, 1993]).
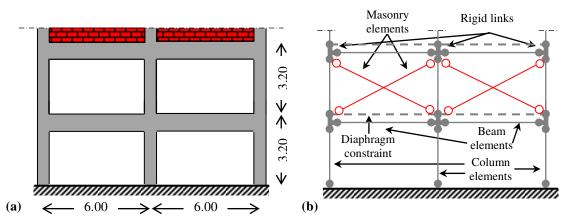

Figure 14. Simulation of the structural system and infills of the examined buildings: (a) layout of structural members and infills; (b) discretization using linear finite elements.

5.3 Selection of the records for performing time-history analyses

Time-history dynamic analyses were carried out utilizing a suite of ten acceleration records from past strong earthquakes that have occurred in Greece between 1978 and 2014. Record datasets were selected from the ITSAK earthquake database [ITSAK, 2016]. From among the ten earthquake records used in the analyses, five were recorded in the near-fault zone (i.e. within 20 km from the rupture fault) and the other five datasets were recorded on sites with a distance from rupture fault ranging from 22 to 40 km. Consideration of both near- and far-fault records was made in order to

account for the effect of ground motion parameters that in some cases can control the performance of structures [Bray and Rodriguez-Marek, 2004; Alavi and Krawinkler, 2004]. The records' characteristics are summarized in Table 5; the absolute acceleration and relative displacement response spectra, S_a and S_d respectively, calculated considering a viscous damping equal to $\xi = 5\%$, are presented in Fig. 15. Each acceleration record was imposed separately in each of the two principal plan directions of the examined building models, except for the cases of buildings belonging to group B, whose seismic response was investigated only for seismic action parallel to the X plan direction, on account of the buildings' double symmetry in plan.

Table 5. Earthquake cases considered in the time-history analyses and their characteristics.

Earthquake	M_L	Station	Epicentral Distance (km)	Record Type	Record Component	PGA (g)
Cephalonia, 03/02/2014	6.1	CHV1	8.85	NF	E	0.755
Aigio, 15/06/1995	5.6	AIGA	21.56	FF	T	0.517
Lefkas, 14/08/2003	5.9	LEF1	< 10	NF	T	0.417
Kalamata, 13/09/1986	5.5	KALA	12.30	NF	T	0.297
Kozani, 13/05/1995	6.1	KOZ1	16.38	NF	L	0.216
Athens, 07/09/1999	5.4	ATH2	19.63	NF	T	0.159
Thessaloniki, 20/06/1978	6.0	THEA	26.35	FF	T	0.150
Alkyonides, 25/02/1981	5.9	KORA	26.55	FF	T	0.137
Kythera, 08/01/2006	6.4	KYT1	> 20	FF	L	0.122
Limnos, 24/05/2014	6.3	LMN1	> 20	FF	E	0.106

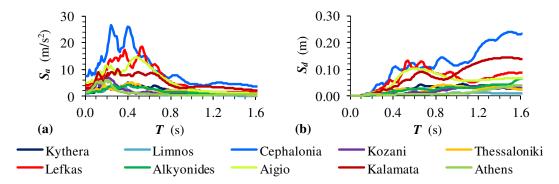NF: Near Fault record, FF: Far Fault record

Figure 15. Response spectra of the earthquake records used in the analyses, calculated for 5% damping: (a) absolute acceleration response spectra; (b) relative displacement response spectra.

5.4 Assessment of the efficiency of the proposed methodology

To test the accuracy and relevance of the proposed procedure for estimating the demands in first storey in non-conforming R.C. buildings, a retrofit scenario was applied in each of the examined buildings in order to control the level of their ID_1 to values lower than 0.5%, i.e., a displacement ductility, $\mu_\delta = 1.0$; this represents the least expensive retrofit option, comprising addition of infill masonry walls in the first storey of the structures. Six bays were infilled parallel to the direction of the seismic excitation as per Fig. 14. Simulation of the 1st storey masonry infills in the building models was achieved similarly to the simulation of masonry infills used for the upper storeys (Fig. 14(b)). The translational stiffness of the infill masonry walls was determined separately for each analysis case. This was achieved by first calculating from the earthquake spectrum (Fig. 15(a)), through the use of Eq. 15, the required stiffness of the first storey, K_1 for a target $ID_1 = 0.5\%$ (i.e. a target ductility of 1). The stiffness contribution of all six masonry infills, $K_{mw,1}$, that would need to be added to the first storey of the examined R.C. building so as to ensure that ID_1 does not exceed the limit of 0.5% in any of the seismic scenarios considered, was calculated from K_1 after the subtraction of the total stiffness contribution of the first storey columns, $K_{c,1}$ (Eq. 2). For each analysis case, the determined value of $K_{mw,1}$ was then equally

distributed among the six infill masonry walls that were added to the initial building model.

Figures 16 – 18 depict the maximum value of ID_1 as this was derived from the results of the time-history dynamic analyses. Each graph of Figs. 16 – 18 presents the maximum lateral interstorey drift ratio response of the first storey of the building models, both at their initial state (light grey triangles) and after having been retrofitted with the addition of the masonry infills (dark grey rhombi). Note that masonry infills in the first storey were added only to those building models where the maximum lateral drift response of the first storey exceeded the target value $ID_1 = 0.5\%$.
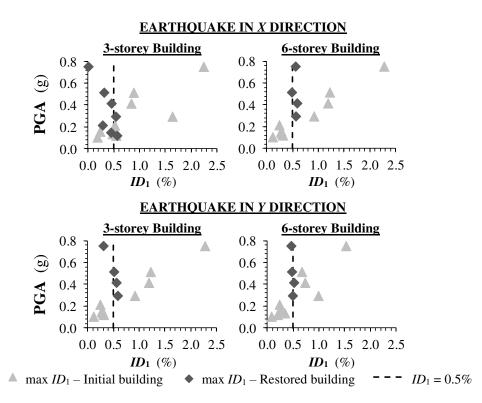

Figure 16. Peak estimated seismic response of buildings belonging to group A, as calculated from time-history dynamic analyses.
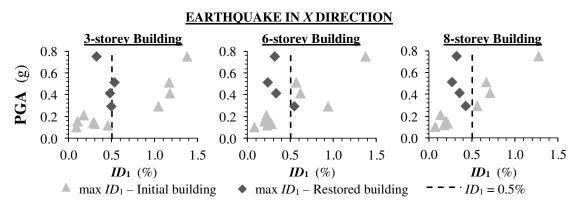
Figure 17. Peak estimated seismic response of buildings belonging to group B, as calculated from time-history dynamic analyses.
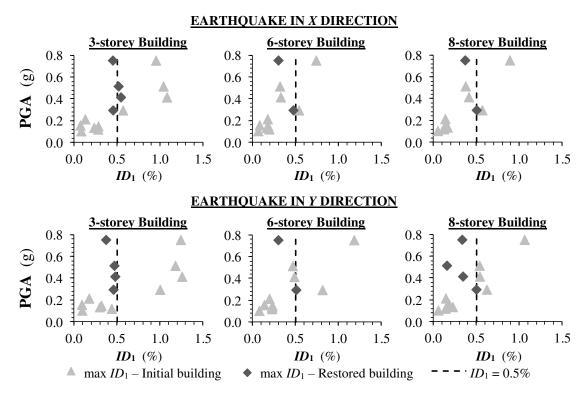

Figure 18. Peak estimated seismic response of buildings belonging to group C, as calculated from time-history dynamic analyses.

As illustrated, the addition of the masonry infills improved the estimated ID_1 values in all the examined cases; among the 49 analyses cases of retrofitted buildings considered, in 5 cases did the maximum value of ID_1 exceed the limit of 0.5%, which was set as target in estimating the required lateral stiffness contribution of masonry infill walls (Eq. 15). However, even in these cases the peak value of ID_1 did not exceed 0.6% (displacement ductility, $\mu_\delta = 1.2$, with assumed yielding at $ID_1 = 0.5\%$,

Priestley et al. 1996), therefore the difference of these analyses results from the limiting value of $ID_1 = 0.5\%$ was within a negligible margin.

The value of improving the seismic response of substandard R.C. buildings with the addition of masonry infills in their soft storey is further demonstrated by comparing the maximum value of the shear forces developing at the examined buildings' first storey columns during the earthquakes, before and after the retrofit, $|max|V_{Initial}$ and $|max|V_{Retrofit}$, respectively. Figure 19 presents the values of $|max|V_{Retrofit}$ developing at the central column of the first storey of each retrofitted building, in the direction of the earthquake excitation, as a percentage of the corresponding value before the retrofit with the addition of masonry infills. As depicted in Fig. 19, the addition of masonry infills lead to significant reduction of the $|max|V_{Retrofit}$, which increases along with the increase of PGA of the earthquake. The most impressive reduction in the value of maximum shear force developing along the first storey central column corresponds to the case of the 8-storey, group C, building subjected to the Cephalonia earthquake. In the case of earthquake action parallel to the X plan direction, the developed shear was reduced from $|max|V_{Initial} = 695.5$ kN to $|max|V_{Retrofit} = 295.9$ kN, whereas the corresponding reduction when the earthquake was imposed in the Y plan direction was reduced by 358.3 kN (i.e. from $|max|V_{Initial} = 526.5$ kN to $|max|V_{Retrofit} = 168.2$ kN).

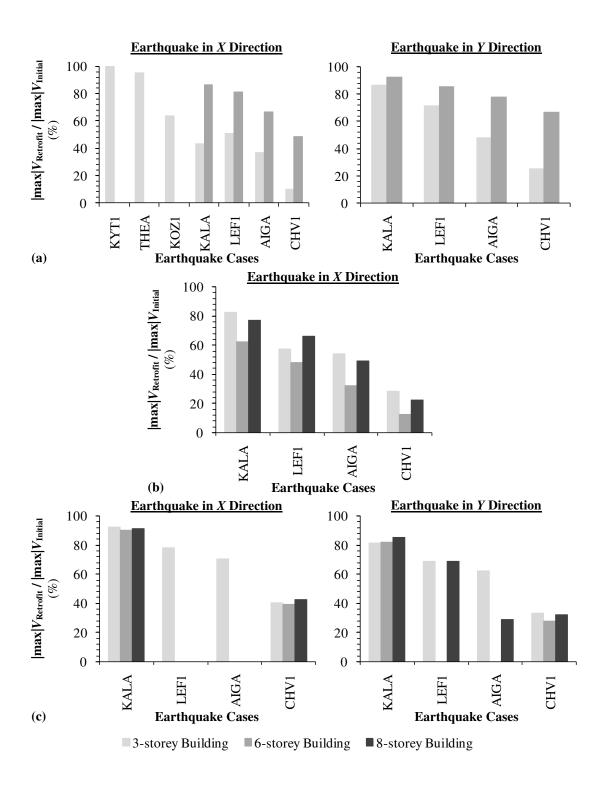Figure 19. Reduction of |max|$V_{Retrofit}$ of the first storey central column of all retrofitted building cases as compared to the corresponding value of |max|$V_{Initial}$: (a) building group A, (b) building group B, (C) building group C.

Also note that the analyses results confirm the safety of evaluating the out-of-

plane seismic response of masonry infills added to the critical floors of an R.C.

building as a retrofit solution (Fig. 5(b)) by considering peak value of spectral acceleration perpendicular to the infills' plane equal to $(L^*/M^*) \cdot S_a$. According to the analyses results, in no case the calculated maximum acceleration developing in the critical floors of the vibrating building models exceeded that limit. An indicative example of storey peak acceleration values, as those where calculated in the cases of both the initial and the retrofitted versions of the 8-storey, group B building, subjected to the Aigio earthquake (PGA = 0.517g) in *X* plan direction, is presented in Table 6.

Table 6. Peak values of calculated absolute accelerations in the floors of the initial and the retrofitted 8-storey, group B building and comparison with the approximated response.

Floor	Initial Building			Retrofitted Building		
	Calculated Peak Absolute Acceleration (g)	Fundamental Mode Shape	$(L^*/M^*) \cdot S_a$ (g)	Calculated Peak Absolute Acceleration (g)	Fundamental Mode Shape	$(L^*/M^*) \cdot S_a$ (g)
8	0.68	1.000	1.60	1.56	1.000	1.69
7	0.58	0.956		1.37	0.923	
6	0.44	0.897		1.12	0.816	
5	0.38	0.822		0.81	0.684	
4	0.37	0.735		0.61	0.531	
3	0.36	0.637		0.47	0.364	
2	0.35	0.531		0.50	0.191	
1	0.29	0.417		0.52	0.023	

In conclusion, the results of the parametric time-history dynamic analyses highlighted the significance of the presented retrofit procedure, in terms of controlling the distribution of interstorey drift demand along the height of the soft storey in pilotis-type, non-conforming, R.C. buildings to a required level, as a means to control the extent of developed damages in the structural elements. It is important to note that the infill-frame interactions are complex in nature and non-linear analysis may be warranted to further support the analytical trends extracted from the linear elastic analysis. Modelling these phenomena would affect the relevance and efficiency of the nonlinear solution as well – clearly, a more complete understanding of the problem

would be obtained if simultaneous correlation between field measurements, linear elastic analyses and nonlinear models, and this effort would have to be undertaken in the future for completeness.

6. Conclusions

Retrofit design of existing reinforced concrete structures that do not conform to the current Code Seismic design standards is imperative in countries with high seismicity, as this category of buildings represents the majority of the building stock. In this framework, simple rehabilitation solutions need be developed that may be used easily by practitioners. The best option is to mitigate localization of deformation through addition of stiffness in potential soft-storeys of R.C. frames. From among the many alternatives to achieve that objective, the most cost effective is through masonry infills in strategically chosen open bays of frames. Furthermore, masonry infills may easily be replaced after damage, and through their low strength they prevent the transfer of large forces in the foundation.

This paper presents a procedure for improved distribution of the interstorey drift demand height-wise in the structure, so as to minimize localization of drifts in the soft storey locations and to control the extent of anticipated damage. The procedure is developed in the form of simple equations and practical design charts, which link drift demand to the area ratios of infills of the critical floors of the structure, so that it may be used easily by practitioners. In using the charts the input design parameter is the maximum tolerable drift demand of the critical floors of the retrofitted structure, which for the design earthquake may be considered up to 0.5%; through this it is possible to determine by reverse engineering the required stiffness addition (by masonry infills) that will secure that the drift limit is not exceeded during the design earthquake. Application and relevance of the proposed procedure is demonstrated

through example case studies of both an actual building that collapsed during the 2008 Andravida earthquake in Greece and a series of time-history dynamic analyses to building models of non-conforming, multistorey, R.C. buildings. The procedure is robust and results are consistent with field observations. However, additional proof-testing against the contribution of the added masonry infills in triggering local shear failures in the adjusted columns is required before this may be used by practitioners as tool in the field.

References

Alavi, B. and Krawinkler H. [2004] "Behavior of moment-resisting frame structures subjected to near-fault ground motions," Earthquake Engineering and Structural Dynamics 33, 687–706.

Bolea, O. [2016] "The Seismic Behaviour of Reinforced Concrete Frame Structures with Infill Masonry in the Bucharest Area," Energy Procedia 85, 60–76.

Bray, J. D. and Rodriquez-Marek A. [2004] "Characterization of forward-directivity ground motions in near-fault region," Soil Dynamics and Earthquake Engineering 24, 815–828.

Brzev, S. [2007] "Earthquake-resistant confined masonry construction," National Information Center of Earthquake Engineering, Indian Institute of Technology, Kanpur, India.

Calvi, G. M. and Bolognini, D. [2001] "Seismic response of reinforced concrete frames infilled with weakly reinforced masonry panels," Journal of Earthquake Engineering 5(02), 153–185.

Chourasia, A., Bhattacharyya, S., Bhandari, N. and Bhargava, P. [2016] "Seismic Performance of Different Masonry Buildings: Full-Scale Experimental Study," Journal of Performance of Constructed Facilities 30(5), 04016006.

Clough, R. W. and Penzien, J. [1993] Dynamics of Structures (2nd edn), MacGraw-Hill Inc., New York.

EN 1992-1-1 [2003] "Eurocode 2 – Design of concrete structures - Part 1-1: General rules and rules for buildings," European Committee for Standardization (CEN), Brussels.

EN 1998-1 [2004] "Eurocode 8 – Design of structures for earthquake resistance - Part 1: General rules, seismic actions and rules for buildings," European Committee for Standardization (CEN), Brussels.

EN 1998-3 [2005] "Eurocode 8 – Design of structures for earthquake resistance - Part 3: Assessment and retrofitting of buildings," European Committee for Standardization (CEN), Brussels.

Fardis, M. N., Carvalho, E., Elnashai, A., Faccioli, E., Pinto, P. and Plumier, A. [2005] Designers' guide to EN 1998-1 and EN 1998-5 Eurocode 8: Design of structures for earthquake resistance. General rules, seismic actions, design rules for buildings, foundations and retaining structures (1st edn), Thomas Telford Ltd.

Federation of Structural Concrete (*fib*) [2003] "Seismic assessment and retrofit of reinforced concrete buildings," *fib* Bulletin 24, State-of-art report prepared by Task Group 7.1

Fiorato, A. E., Sozen, M. A. and Gamble, W. L. [1970] "An investigation of the interaction of reinforced concrete frames with masonry filler walls," Technical Report, Dept. of Civil Engineering, University of Illinois, Urbana, Illinois.

Greek Code for Interventions (GRECO) [2013], Earthquake Planning and Protection Organization, Athens, Greece.

Haldar, P., Singh, Y. and Paul, D. K. [2013] ''Identification of seismic failure modes of URM infilled RC frame buildings,'' Engineering Failure Analysis 33, 97–118.

Hashemi, S. A. and Mosalam, K. M. [2007] ''Seismic evaluation of reinforced concrete buildings including effects of infill masonry walls,'' Pacific Earthquake Engineering Research Center, PEER, 100, 1026–1037.

Hashemi, A. and Mosalam, K. M. [2006] "Shake-table experiment on reinforced concrete structure containing masonry infill wall," Earthquake Engineering and Structural Dynamics 35(4), 1827–1852.

Hossein, M. and Kabeyasawa, T. [2004] ''Effect of infill masonry walls on the seismic response of reinforced concrete buildings subjected to the 2003 Bam earthquake strong motion: a case study of Bam telephone center,'' Bull. Earthquake Research Institute - Univ. Tokyo 79, 133-156.

Huang, Q., Guo, Z. and Kuang, J. S. [2016] ''Designing infilled reinforced concrete frames with the 'strong frame-weak infill' principle,'' Engineering Structures 123, 341–353.

Institute of Engineering Seismology and Earthquake Engineering – ITSAK [2016] Earthquake Database, Thessaloniki, Macedonia, Greece, available from: http://itsak.gr.

Institute of Engineering Seismology and Earthquake Engineering – ITSAK [2008] "Report on the 8-6-2008, M6.5, Achaia-Ilia earthquake," Thessaloniki, Macedonia, Greece, available from: http://itsak.gr (in Greek).

Kakaletsis, D. and Karayannis, C. [2007] ''Experimental investigation of infilled R/C frames with eccentric openings,'' Structural Engineering and Mechanics 26(3), 231–250.

Karantoni, F. V., Papadopoulos, M. and Pantazopoulou, S. J. [2016] "Simple seismic assessment of traditional unreinforced masonry buildings," International Journal of Architectural Heritage 10(8), 1055-1077.

Korkmaz, S. Z., Kamanli, M., Korkmaz, H. H., Donduren, M. S. and Cogurcu, M. T. [2010] ''Experimental study on the behaviour of nonductile infilled RC frames strengthened with external mesh reinforcement and plaster composite,'' Natural Hazards and Earth System Sciences 10(11), 2305–2316.

Kyriakides, M. A. and Billington, S. L. [2014] "Cyclic Response of Nonductile Reinforced Concrete Frames with Unreinforced Masonry Infills Retrofitted with Engineered Cementitious Composites," Journal of Structural Engineering 140(2), 04013046.

Li, B., Wang, Z., Mosalam, K. M. and Xie, H. [2008] ''Wenchuan earthquake field reconnaissance on reinforced concrete framed buildings with and without masonry infill walls,'' Proc. of the 14th World Conference on Earthquake Engineering, Beijing, China.

Matosevic, D., Sigmund, V. and Guljas, I. [2015] "Cyclic testing of single bay confined masonry walls with various connection details," Bull Earthquake Eng 13, 565–586.

Mehrabi, A. B., Benson Shing, P., Schuller, M. P. and Noland, J. L. [1996] ''Experimental evaluation of masonry-infilled RC frames,'' Journal of Structural Engineering 122(3), 228–237.

Misir, I. S., Ozcelik, O. Girgin, S. C. and Yuse,l U. [2016] "The Behavior of Infill Walls in RC Frames Under Combined Bidirectional Loading," Journal of Earthquake Engineering 20(4), 559–586.

Model Code 2010 [2010], "*fib* Model Code for Concrete Structures 2010," International Federation for Structural Concrete (*fib*), Lausanne, Switzerland.

Murty C. V. R. and Jain, S. K. [2000] "Beneficial influence of masonry infill walls on seismic performance of RC frame buildings," Proc. of the 12th World Conference on Earthquake Engineering, Auckland, New Zealand.

Negro, P. and Verzeletti, G. [1996] "Effect of infills on the global behavior of R/C frames: Energy considerations from pseudodynamic tests," Earthquake Engineering and Structural Dynamics 25(8), 753–773.

Open System for Earthquake Simulation (OpenSees) [2016], Pacific Earthquake Engineering Research Center – PEER, Berkeley, CA, Available from: http://peer.berkeley.edu/OpenSees.

Ozkaynak, H., Yuksel, E., Yalcin, C., Dindar, A. A. and Buyukozturk, O. [2014] "Masonry infill walls in reinforced concrete frames as a source of structural damping," Earthquake Engineering and Structural Dynamics 43(7), 949–968.

Pantazopoulou, S. J., Tastani, S., Thermou, G. and Triantafyllou, T. [2016] "Background to European seismic design provisions for the retrofit of R.C. elements using FRP materials," FIB Structural Concrete 17(2), 194–219.

Pardalopoulos, S., Thermou, G. E. and Pantazopoulou, S. J. [2013] "Preliminary seismic assessment method for identifying R.C. structural failures," Computational Methods in Earthquake engineering, Computational Methods in applied sciences 30, 111–128.

Pardalopoulos, S., Thermou, G. E. and Pantazopoulou, S. J. [2013] "Screening criteria to identify brittle R.C. structural failures in earthquakes," Bulletin of Earthquake Engineering 11, 607–636.

Perez Gavilan, J. J., Flores, L. E. and Alcocer, S. M. [2015] "An Experimental Study of Confined Masonry Walls with Varying Aspect Ratios," Earthquake Spectra 31(2), 945–968.

Priestley, M. J. N., Seible F., Calvi G.M. [1996] Seismic design and retrofit of bridges, John Wiley & Sons, Inc., New York.

Pujol, S., Benavent-Climent, A., Rodriguez, M. E. and Smith-Pardo, J. P. [2008] "Masonry infill walls: an effective alternative for seismic strengthening of low-rise reinforced concrete building structures," Proc. of the 14th World Conference on Earthquake Engineering, Beijing, China.

Rajesh C., Pradeep-Kumar R., and Kandru S., [2014], "Seismic Performance of RC Frames Buildings With and Without Infill Walls", Intnl. J. of Engineering Research & Technology, (IJERT), ISSN:2278-0181, 3(10).

Serrato, F. and Saatcioglu, M. [2004] "Seismic Retrofit of Masonry Infill Walls in RC Frames," Report OCCERC 04–31.

Sigmund, V. and Penava, D. [2013] "Assessment of masonry infilled reinforced-concrete frames with openings," Technical Gazette 20(3), 459–466.

Stavridis, A., Koutromanos, I. and Shing, P. B. [2012] "Shake-table tests of a three-story reinforced concrete frame with masonry infill walls," Earthquake Engineering and Structural Dynamics 41(6), 1089–1108.

Su, Q., Cai, G. and Cai, H [2016] "Seismic behaviour of full-scale hollow bricks-infilled RC frames under cyclic loads," Bulletin of Earthquake Engineering, 1–32.

Thermou, G. E., Pantazopoulou, S. J. and Elnashai, A. S. [2012] "Global interventions for seismic upgrading of substandard R.C. buildings," Journal of Structural Engineering 138(3), 387–401

Thermou, G. E., Elnashai, A. S. and Pantazopoulou, S. J. [2012] "Retrofit yield spectra – A practical device in seismic rehabilitation," Earthquake and Structures 3(2), 141–168.

Thermou, G. E. and Pantazopoulou, S. J. [2011] "Assessment indices for the seismic vulnerability of existing R.C. buildings," Earthquake Engineering and Structural Dynamics 40(3), 293–313.

Varum, H. [2003] "Seismic assessment, strengthening and repair of existing buildings," Ph.D. thesis, Universidade de Aveiro.

Verderame, G. M., Ricci, P., Del Gaudio, C. and De Risi, M. T. [2016] "Experimental tests on masonry infilled gravity-and seismic-load designed RC frames," Proc. of the 16th International Brick and Block Masonry Conference, Padova, Italy.

Yeh, Y. H. and Liao, W. I. [2005] "Cyclic performance of two-story ductile RC frames with infill walls," Proc. of the ASME 2005 Pressure Vessels and Piping Conference, American Society of Mechanical Engineers, pp. 259–264